

Heat Transfer and Fluid Flow Characteristics of Three Sides Artificially Roughened and Glass Covered Solar Air Heaters

Ashwini Kumar¹, B. N. Prasad², K. D. P. Singh³

¹Research Scholar, Mechanical Engineering Department, N.I.T, Jamshedpur, India-831014

²Professor, Mechanical Engineering Department, N.I.T, Jamshedpur, India-831014

³Associate professor, Mechanical Engineering Department, N.I.T, Jamshedpur, India-831014

Email address: ashu448[AT]gmail.com

Abstract— An experimental investigation for the flow region ($8 < e^+ < 35$), has been carried out for the results of heat transfer coefficient and friction factor in three sides artificially roughened and glass covered solar air heater, simultaneously with three sides glass covered smooth ones. The effects of relative roughness height (e/D) and relative roughness pitch (p/e) on Nusselt number and friction factor have been studied, covering the Reynolds number range of 4000-20000, for a fixed duct aspect ratio of 8. Based on the experimental results, correlations of Nusselt number and friction factor have been developed as a function of flow and roughness parameters. A good agreement has been found between the predicted and experimental values with a maximum average deviations of $\pm 12\%$ and $\pm 11\%$, respectively.

Keywords— Nusselt number, friction factor, roughness reynolds number, reynolds number, three sides artificial roughness.

Nomenclature

A_C absorber plate area, m^2
 A_2 throat area of orifice meter, m^2
 B solar air heater duct height, m
 C_p specific heat of air at constant pressure, $kJ/kg\cdot K$
 C_d coefficient of discharge
 D hydraulic diameter of solar air heater duct, m
 e roughness height, m
 e/D relative roughness height
 e^+ roughness Reynolds number, $e^+ = \frac{e}{D} \sqrt{\frac{f_r}{2}} Re$
 f friction factor
 f_s friction factor in three sides glass covered smooth collector
 f_{3r} friction factor in three sides roughened and glass covered collector
 g acceleration due to gravity, m/s^2
 h convective heat transfer coefficient, $W/m^2\cdot K$
 I intensity of solar radiation, W/m^2
 K thermal conductivity of G.I. sheet, $W/m\cdot K$
 L length of test section, m
 \dot{m} mass flow rate, kg/s
 Nu Nusselt number
 Nu_{3r} Nusselt number in three sides roughened and glass covered collector

Nu_s Nusselt number in three sides glass covered smooth collector
 p roughness pitch, m
 p/e relative roughness pitch
 P_r Prandtl number
 Re Reynolds number
 SWG Standard wire gauge
 T_a ambient temperature of air, K
 \bar{T}_f average temperature of air, K
 T_f fluid (air) temperature, K
 T_i inlet temperature of air, K
 T_o outlet temperature of air, K
 V air velocity in duct, m/s
 W width of solar air heater duct, m
 ρ density of air, kg/m^3
 β_1 ratio of throat diameter of orifice meter to flow pipe diameter

I. INTRODUCTION AND LITERATURE REVIEWS

The provision of an artificial roughness of different configurations have been used in plenty of studies to enhance the heat transfer rate in solar air heaters during the last decades. Varying magnitudes of roughness results in varying values of heat transfer and friction factor enhancement. An enhancement of about double than that of smooth solar air heater with respect to heat transfer coefficient have been reported (Prasad and Saini, 1988; Prasad, 2013), while the friction factor quadrupled. Heat transfer and friction factor correlations have been obtained for V-rib roughened solar air heaters (Hans et al., 2010). The effect of different orientation of W-rib roughness has been investigated to enhance heat transfer in solar air heaters (Lanjewar et al., 2011). Review reports on roughness geometries used in solar air heaters are available (Varun et al., 2007; Shakya et al., 2013). CFD based analysis for heat transfer and friction factor has been made for transverse wire roughness in solar air heaters (Yadav and Bhagoria, 2013). Nusselt number and friction factor correlations have been obtained for arc-shaped wire roughness and dimple shaped roughness (Saini and Saini, 2008; Saini and Verma, 2008). Reviews (Chamoli et al., 2012; Gawande et al., 2014) for turbulence promoters and effect of roughness geometries on heat transfer enhancement in solar thermal

systems give wide range of data and results on heat transfer and friction factor.

Artificial roughness provided on absorber plates invariably enhances heat transfer associated with increase in friction factor. Increase in heat transfer increases the thermal performance but increase in friction factor affects the thermo hydraulic performance. Thermal and thermo hydraulic performance results of roughened solar air heaters have been reported (Bhushan and Singh, 2012; Chabane et al., 2014; Saurav and Sahu, 2013; Varun et al., 2008). Effect of the roughness parameters (p/e , e/D) and Reynolds number have been represented and discussed in literature to a large extent to arrive at conclusion that increasing values of e/D for a given value of p/e increases heat transfer and friction factor both.

Despite plenty of works dealing with the effect of artificial roughness on heat transfer and friction factor in solar air heaters, very few dealt with the thermo hydraulic performance in them. Based on the approach adopted (Sheriff and Gumley, 1966; Lewis, 1975; Webb and Eckert, 1977), analysis for the optimal thermo hydraulic performance in one side roughened solar air heater has been reported (Prasad and Saini, 1991). They obtained the value of roughness Reynolds number, $e^+ = 24$, for optimal thermo hydraulic condition. Results on thermal and thermo hydraulic performance of wavy finned absorber plate solar air heaters have been reported recently (Priyam and Chand, 2016).

However, in all the above cases, provision of artificial roughness and glass cover has remained limited to only one side (top side) of the solar air heater duct except those of the recent ones (Prasad et al., 2014; Kumar et al., 2016a, Behura et al., 2016; Behura et al., 2017), wherein it has been concluded that three sides roughened and glass covered solar air heaters perform even better than those of one side roughened and glass covered solar air heaters, but friction factor also increases. The effect of glass cover has been shown (Kumar et al., 2016b) by performing an investigation, that has given even better performance for three sides glass covers as compared to that of the one side glass covered one. The authors (Prasad et al., 2015), analysis could reveal that, $e_{opt}^+ = 23$, corresponds to the optimal thermo hydraulic performance in three sides artificially roughened and glass covered solar air heaters, which have further been verified by taking an experimental investigation (Kumar et al., 2017)

The present paper deals with the experimental results obtained with respect to heat transfer and friction factor for three sides roughened and glass covered solar air heater, along with the three sides glass covered smooth ones. The effect of roughness and flow parameters on Nusselt number and friction factor have been shown for the range of investigated parameters. On the basis of experimental data, the correlations of heat transfer and friction factor for three sides artificially roughened (rectangular with three sides wire) and glass covered solar air heater have been developed.

II. METHODOLOGY

The experimental set-up consists of two solar air heater ducts both having aspect ratio value of 8 and similar size : (i)

smooth with three sides glass covers and (ii) three sides roughened with three sides glass covers as shown in Figs. 1(a) and (b). Fig. 2(a), (b) and (c) show the schematic, pictorial and top view of the experimental set-up respectively with measuring instruments and run by a single 5 HP blower simultaneously. Mass flow rate was varied by controlling the blower speed by means of a 3-phase auto variac and measured by means of two separate flange tape orifice-meters having discharge coefficient of 0.61. Multi-tube manometers were used to measure the pressure drop along the duct length. Pressure taps as shown in Fig. 3, connected to multitube manometer by means of PVC tubes measured the pressure drop along the collector duct length. Air and plate temperatures were measured by means of 28 SWG copper-constant on thermocouples fed to digital sensors. Intensity of solar radiation was measured by a digital pyranometer, installed at the experiment site. Thermocouple arrangement for the plate temperature measurement has been shown in Fig. 4.

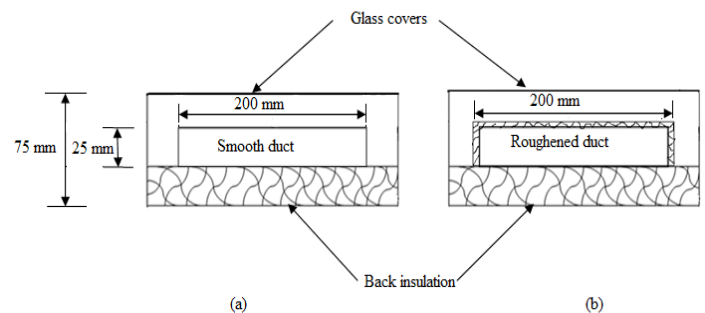
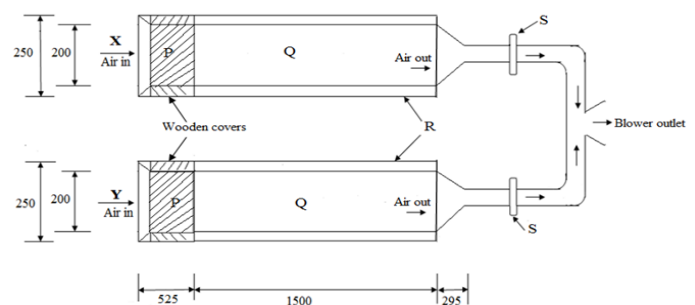


Fig. 1. (a) and (b) Solar air heater duct models.



All dimensions are in mm

- X- Three sides roughened and glass covered solar air heater
- Y- Smooth and three sides glass covered solar air heater
- P- Unheated wooden covered entry section
- Q- Glass covered test section
- R- Glass covers
- S- Flange tape orifice-meters

Fig. 2(a). Schematic diagram of the experimental set-up.

Test data were obtained outdoor on the roof of a building on clear sky days between 11 AM and 2 PM during the months of February to May 2015. A wide range of experimental data for 105 number of test runs for 15 set of roughened absorber plates were collected simultaneously with the smooth one. The roughness and flow parameters were selected so as to yield a wide range of values of the roughness

Reynolds number, e^+ On a single day, test data were collected for a given value of mass flow rate. Table I shows the range of parameters investigated.

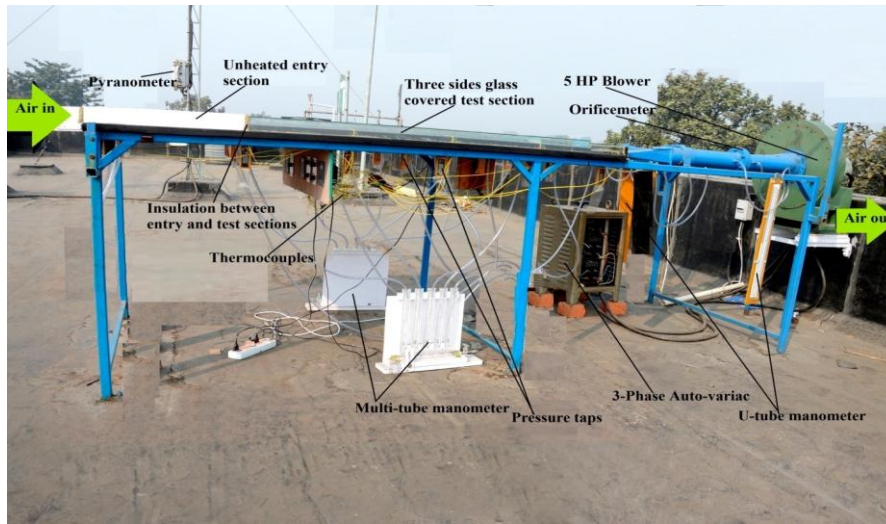


Fig. 2(b). Pictorial view of the experimental set-up.

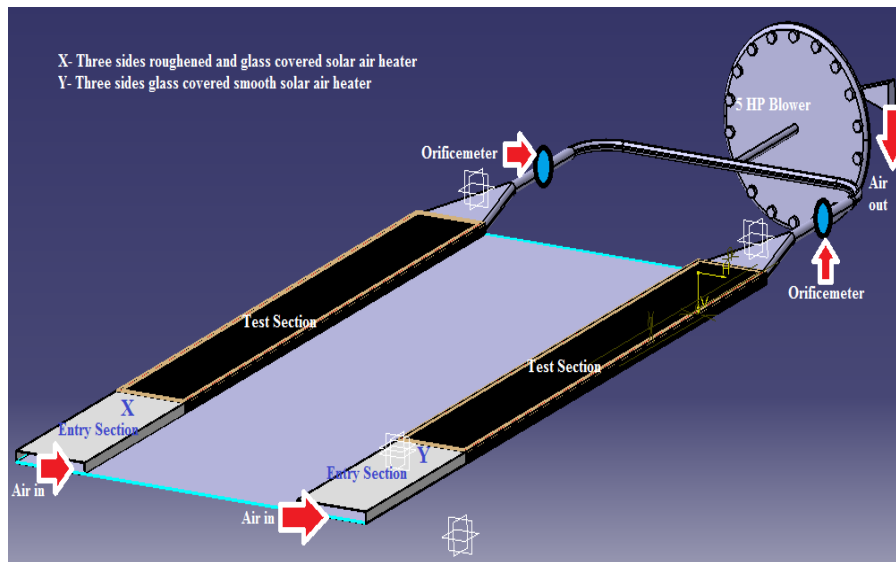


Fig. 2(c). Top view of the experimental set-up.

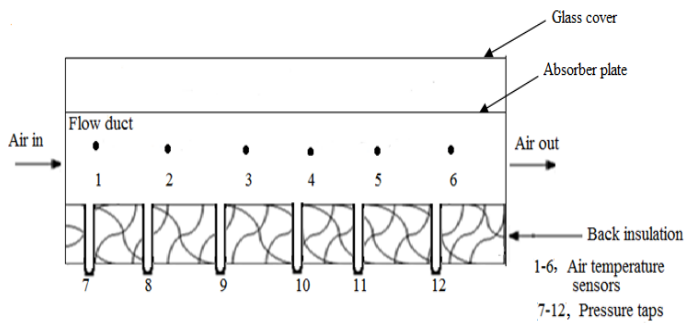


Fig. 3. Arrangement of air temperature sensors and pressure taps along the duct length.

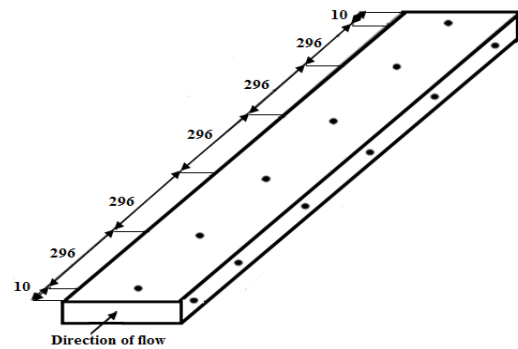


Fig. 4. Thermocouple arrangement on top and side absorber plate. Dimensions are in mm

TABLE I. Range of parameters investigated.

Sl. No	Parameters	Range
1.	Mass flow rate, kg/s	$8.35 \times 10^{-3} - 3.75 \times 10^{-2}$
2.	Reynolds number, Re	4000 – 20000
3.	Roughness height, mm	0.5 – 1.2
4.	Roughness pitch, mm	6 – 30
5.	Relative roughness pitch, p/e	10 – 30
6.	Relative roughness height, e/D	0.0130 – 0.0250
7.	Roughness Reynolds number, e^+	8 – 35
8.	Intensity of solar radiation, I , W/m^2	699 – 899
9.	Absorber plate length, L , mm (fixed)	1500
10.	Duct width, W , mm (fixed)	200
11.	Duct height, B , mm (fixed)	25

III. DATA REDUCTION AND PRESENTAION

Table II, showing typically the variation of intensity of solar radiation and ambient temperature is represented by Fig.

TABLE II. Typical variation of ambient temperature and intensity of solar radiation during a day.

Time (Hrs.)	11.00	11.15	11.30	11.45	12.00	12.15	12.30	12.45	13.00	13.15	13.30	13.45	14.00
I , W/m^2	786	790	795	801	811	844	877	899	759	742	720	699	648
T_a , $^{\circ}C$	32.9	32.9	33.4	34.1	33.4	33.8	34.1	34.4	34.5	34.6	34.7	34.8	36.1

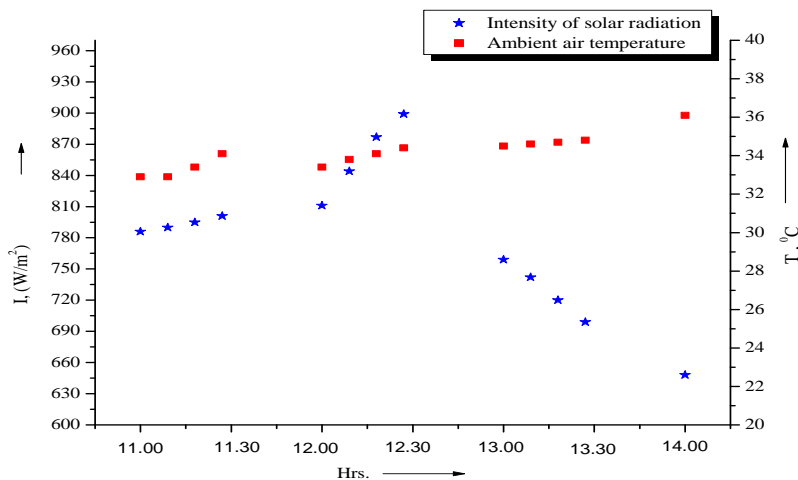


Fig. 5. Typical variation of solar radiation and ambient temperature on a day.

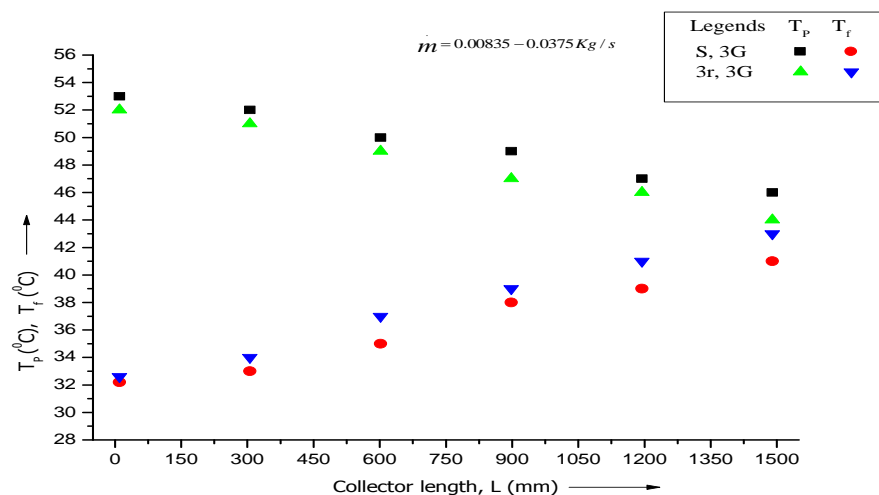


Fig. 6. Instantaneous air and plate temperature in solar air heaters.

5. Fig. 6 shows the instantaneous plate and air temperature in three sides roughened and smooth solar air heaters, across the collector length. Fig. 6 shows that the plate temperature in smooth solar air heater is more than that in three sides roughened one, but air temperature in three sides roughened solar air heater is more than that in smooth one. Higher values of plate temperature and lower values of air temperature in three sides glass covered smooth solar air heater than those in three sides roughened and glass covered solar air heater indicate higher rate of heat transfer in three sides roughened collector than that in smooth collector. Table III shows the typical raw experimental data.

TABLE III. Raw experimental data of fluid temperature.

Time (Hrs.)	T _a , °C	Configuration	T ₁₁		T ₁₂		T ₁₃		T ₁₄		T ₁₅		T ₁₆		T ₁₇	
			T	S	T	S	T	S	T	S	T	S	T	S	T	S
11.00	32.9	3r	33	33	34	34	35	35	37	36	36	36	38	38	39	39
		smooth	33	33	33	33	33	34	34	34	34	35	34	34	35	35
11.30	33.4	3r	34	34	35	36	36	36	37	37	38	37	39	40	41	41
		smooth	34	34	34	34	34	35	35	35	35	36	37	38	38	38
12.00	33.4	3r	34	34	36	36	36	35	36	36	37	39	40	40	41	42
		smooth	34	34	34	34	35	35	35	35	35	36	37	38	38	39
12.30	34.1	3r	34.4	34.2	35	34.1	35	35	38	39	40	41	41	41	42	42
		smooth	34.1	34.2	34.5	34.6	35	35	36	36	37	37	38	38	38	38
13.00	34.5	3r	35	35	35	36	37	37	38	39	40	40	42	41	42	43
		smooth	35	35	35	35	36	36	36	37	37	38	38	38	38	39
13.30	34.7	3r	35	36	36	37	37	37	39	40	41	41	43	43	45	44
		smooth	35	35	35	36	35	36	37	38	37	37	38	38	38	38
14.00	36.1	3r	36.5	36.8	37	37	38	38	38	39	42	42	44	44	46	45
		smooth	36.2	36.1	36.5	36.9	37	37	37	38	39	39	39	39	42	42

The experimental data with respect to the relative roughness height, relative roughness pitch, flow Reynolds number, intensity of solar radiation, plate and air temperatures, pressure drops along the duct length and orifice-meter have been reduced to obtain the results, using the relevant expressions. The experimental values of heat transfer coefficient have been obtained using the following Eq.(1):

$$m C_p (T_0 - T_i) = h A_c (\bar{T}_p - \bar{T}_f) \tag{1}$$

where, the values of mass flow rate, \dot{m} , have been worked out by using Eq.(2), written under:

$$m = C_d A_2 \left[\frac{2\rho(\Delta P)}{1 - \beta_1^4} \right]^{1/2} \tag{2}$$

where, ΔP is the pressure drop in the orificemeter.

The values of heat transfer coefficient, h , have been further used to calculate the values of Nusselt number by the following Eq.(3):

$$Nu = \frac{hD}{K} \tag{3}$$

The experimental values of friction factor, f_{3r} , have been worked out by the following Eq. (4), written under:

$$f = \frac{\Delta P(2gD)}{4\rho fLv^2} \tag{4}$$

where, ΔP is the pressure drop between the inlet and outlet of the collector length.

Based on the approach adopted (Holman, 2007), for the uncertainty analysis and the errors found in the experimental measurements with different measuring instruments, uncertainties in the calculated values of Nusselt number, friction factor, Reynolds number, thermocouples and orifice-meter have been estimated as $\pm 1.72\%$ to $\pm 6.21\%$, $\pm 1.81\%$ to $\pm 3.67\%$, $\pm 1.53\%$ to $\pm 2.21\%$, $\pm 1.05\%$ to $\pm 1.54\%$ and $\pm 1.03\%$ to $\pm 1.68\%$, respectively.

IV. VALIDATION OF PRESENT INVESTIGATION

The values of Nu and f obtained from experimental data for smooth solar air heater have been compared to the values obtained from Dittus-Boelter equation for Nu and modified Blasius equation for f , which are reproduced below, written under as the following Eqs. (6) and (7):

$$Nu_s = 0.023 Re^{0.8} P_r^{0.4} \text{ (Dittus-Boelter equation)} \tag{6}$$

$$f_s = 0.085 Re^{-0.25} \text{ (Modified Blasius equation)} \tag{7}$$

Comparison of predicted and experimental values of Nusselt number and friction factor has been shown in Figs. 7 and 8, respectively. The average deviations of experimental values of Nu and f from the values predicted by Eqs. (6) and (7), have been found to be ± 2.7 and ± 2.5 , respectively, that shows a good agreement between the two sets of values, ensuring the accuracy of the present data collected with the experimental set-up.

V. RESULTS AND DISCUSSIONS

The present section deals with the effect of roughness and flow parameters on Nusselt number and friction factor for flow air in rectangular channel, embedded with three undersides roughness elements. Figs. 9 and 10 represent the experimental results for Nusselt number in three sides roughened and smooth collectors. It could be seen from these figures that the values of Nusselt number in three sides roughened collector increases with decreasing values of relative roughness pitch, p/e , for a given value of relative roughness height, e/D and increasing values of relative roughness height, e/D , for a given value of relative roughness pitch, p/e , with a monotonous increase in the values of flow Reynolds number, Re . However, for three sides roughened collectors, the values of Nusselt number are found to enhanced by 60% to 114% than those of three sides glass covered smooth collector.

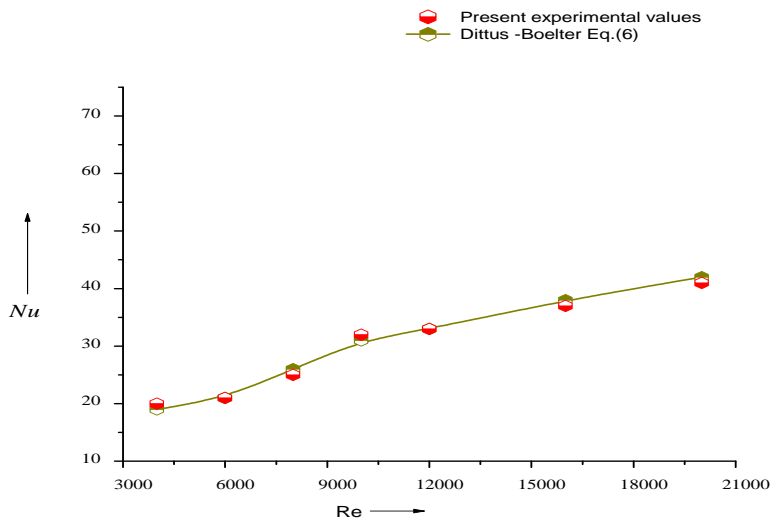


Fig. 7. Validity curve for experimental values of Nusselt number.

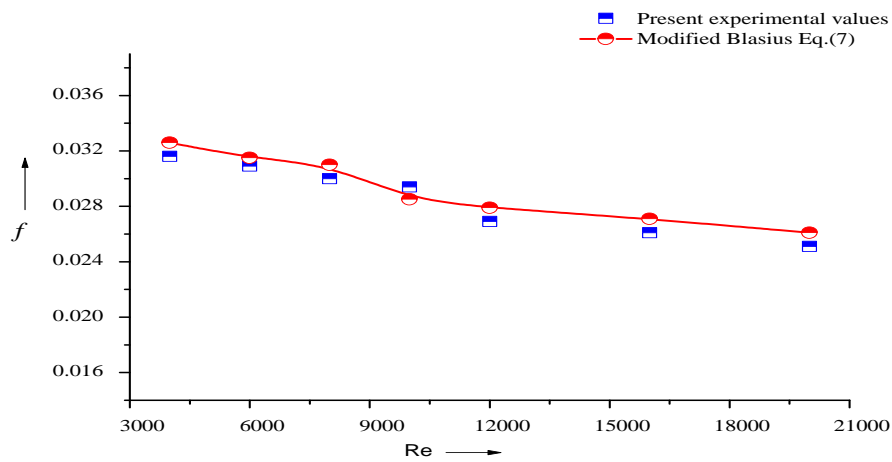


Fig. 8. Validity curve for experimental values of friction factor.

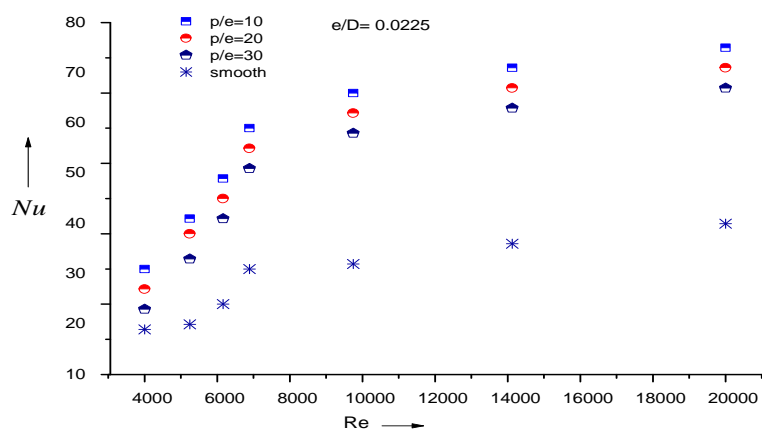


Fig. 9. Effect of p/e on heat transfer in three sides artificially roughened solar air heater.

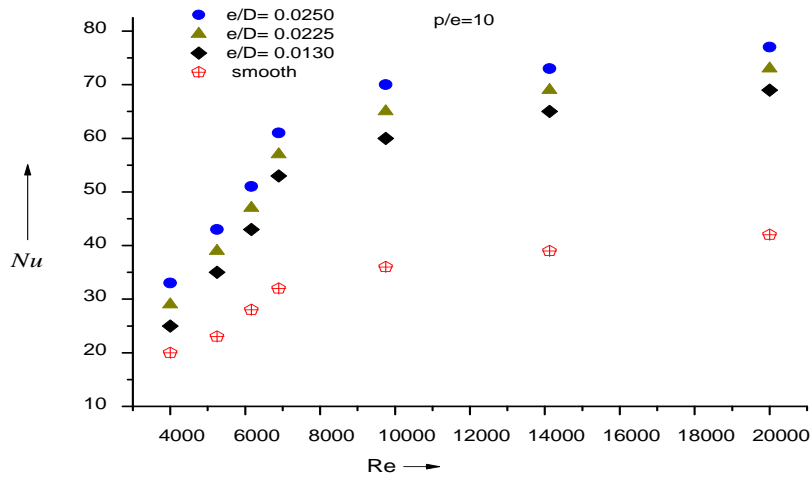


Fig. 10. Effect of e/D on heat transfer in three sides artificially roughened solar air heater.

Figs. 11 and 12 represent the results w.r.t. friction factor for three sides roughened and the smooth one for given value of e/D and p/e , respectively. Fig. 11 shows the effect of p/e on friction factor for a given value of e/D , equal to 0.0225. It could be seen from the figure that the values of friction factor increase with decrease in the value of the relative roughness pitch, p/e , decrease with increasing values of the flow Reynolds number, Re for three sides roughened collector and the smooth ones. The maximum value of friction factor were found at the lowest value of p/e equal to 10. The reason behind it is that, the maximum number of reattachment points is formed at relative roughness pitch p/e of 10 which in turn increases the friction losses. As the

relative roughness pitch (p/e) goes on increasing the number of wires get reduced which in turn results in lower friction losses.

Similarly, Fig. 12 shows the effect of e/D on friction factor for a given value of p/e , equal to 10. It is quite clear from the figure that the values of friction factor increase with the increase in the value of relative roughness height, e/D and the values of friction factor decrease with monotonous increase in the values of flow Reynolds number, Re for three sides artificially roughened collector and the smooth ones. The values of friction factor in three sides roughened collector have been found to increase in the range of 28% to 38%, as compared to the smooth ones.

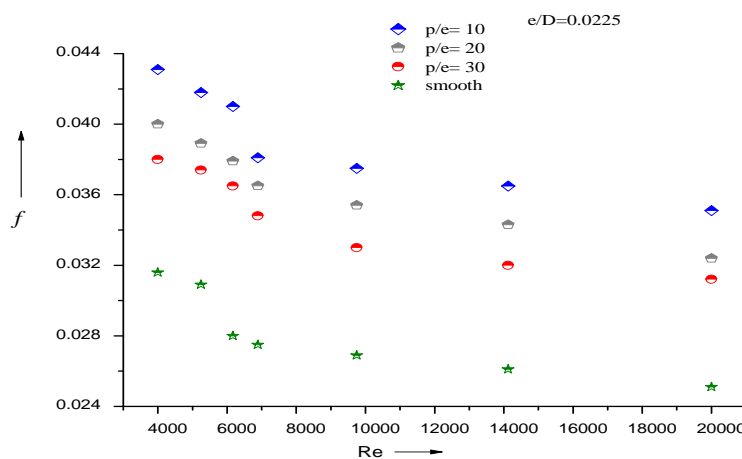


Fig. 11. Effect of p/e on friction factor in three sides artificially roughened solar air heater.

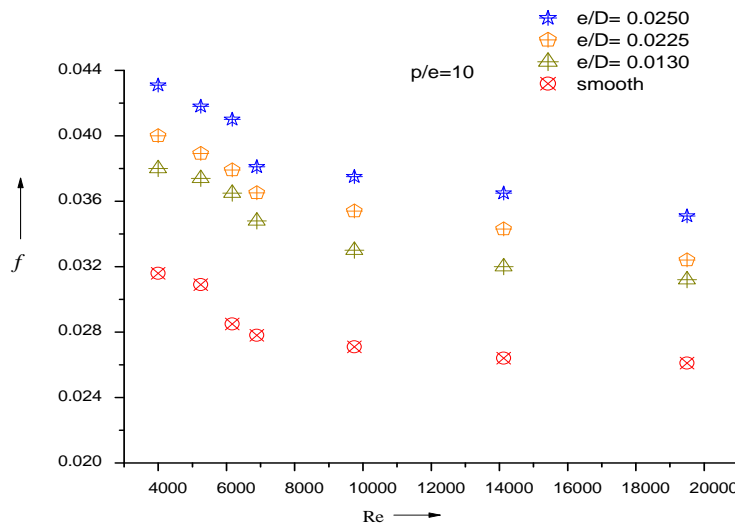


Fig. 12. Effect of e/D on friction factor in three sides artificially roughened solar air heater.

VI. DEVELOPMENT OF CORRELATIONS FOR NUSSELT NUMBER AND FRICTION FACTOR

On the basis of experimental data of heat transfer and friction factor, the correlations for three sides roughened and glass covered solar air heaters, have been developed by using the method of regression analysis, as a function of roughness and flow parameters. A correlation for heat transfer of three sides glass covered smooth solar air heater has also been developed. Since, Nusselt number and friction factor are the strong function of roughness and flow characteristics, viz., flow and roughness parameters, the following functional relationship for Nu_{3r} , Nu_s and f_{3r} can be written as:

$$Nu_{3r} = f_1\left(Re, \frac{p}{e}, \frac{e}{D}\right) \tag{8}$$

$$Nu_s = f_2\left(Re, P_r, f_s\right) \tag{9}$$

$$f_{3r} = f_3\left(Re, \frac{p}{e}, \frac{e}{D}\right) \tag{10}$$

6.1 Correlations for Nusselt Number of Three Sides Roughened and Glass Covered Solar Air Heater

In order to determine a functional relationship between Nu and Re , all the experimental values of Nusselt number, for $e^+ \leq 23$, were plotted against entire range of Reynolds number, as shown in Fig. 13. The well-known regression analysis method for forced convective heat transfer has been utilized to determine the functional equation, written under as:

$$Nu_{3r} = A_0 (Re)^{0.746} \tag{11}$$

Where, A_0 is the function of relative roughness pitch (p/e)

$$\left[A_0 = \frac{Nu_{3r}}{(Re)^{0.746}} \right], \text{ is plotted against all the experimental values}$$

of p/e , as shown in Fig. 14. The regression analysis to fit a straight line through these points has been given by:

$$\frac{Nu_{3r}}{(Re)^{0.746}} = B_0 (p/e)^{-0.0713} \tag{12}$$

Where, B_0 is the function of relative roughness height

$$(e/D) \cdot \left[B_0 = \frac{\frac{Nu_{3r}}{(Re)^{0.746}}}{(p/e)^{-0.0713}} \right], \text{ is plotted against entire}$$

experimental values of e/D , as shown in Fig. 15. The regression analysis to fit a straight line through these points, yield the following correlation for Nusselt number of three sides roughened and glass covered solar air heaters for $e^+ \leq 23$:

$$Nu_{3r} = 0.1415 (p/e)^{-0.0713} (e/D)^{0.0871} (Re)^{0.746} \tag{13}$$

Similarly, the correlation for Nusselt number corresponding to ($e^+ > 23$), were developed by using the method, same as that of above. Figs. (16-18), show the plots between the obtained results, whenafter, applying regression analysis method the following correlation for Nusselt number for three sides roughened and glass covered solar air heaters corresponding to $e^+ > 23$, were developed:

$$Nu_{3r} = 0.0422 (p/e)^{-0.0461} (e/D)^{0.0375} (Re)^{1.208} \text{ for } e^+ > 23 \tag{14}$$

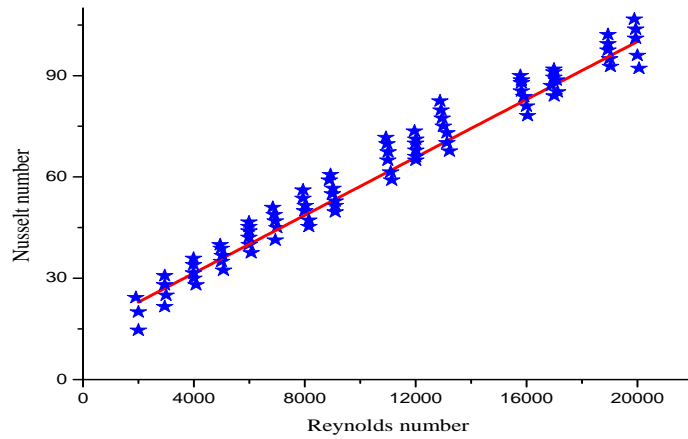


Fig. 13. Variation of Nusselt number with Reynolds number.

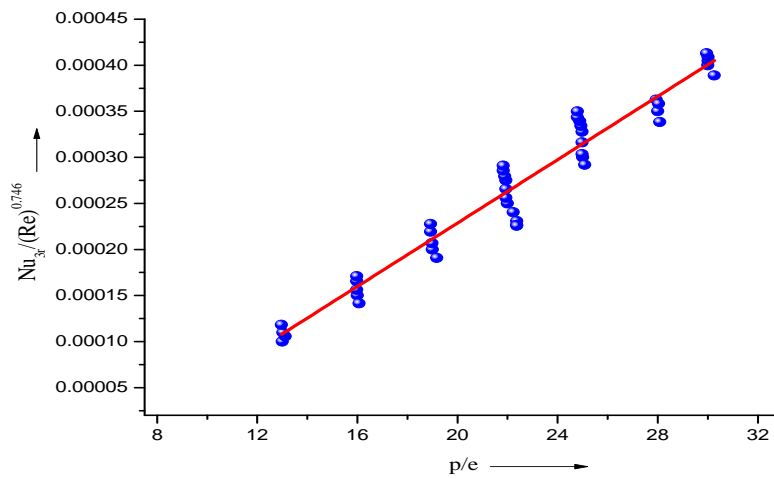


Fig. 14. Plot of $\frac{Nu_{3r}}{(Re)^{0.746}}$ Vs p/e .

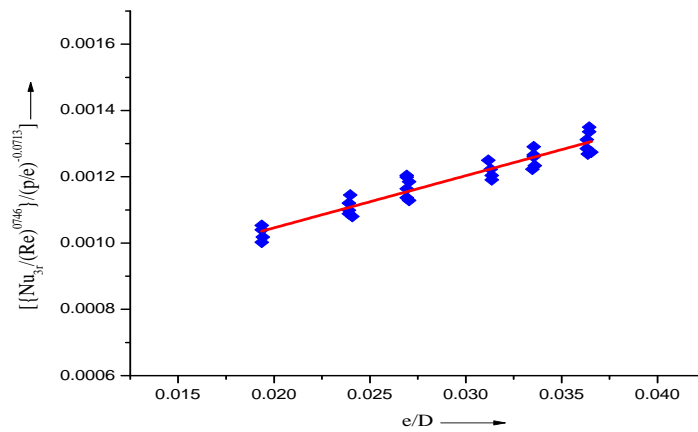


Fig. 15. Plot of $\frac{Nu_{3r}}{(Re)^{0.746}} / (p/e)^{-0.0713}$ Vs e/D .

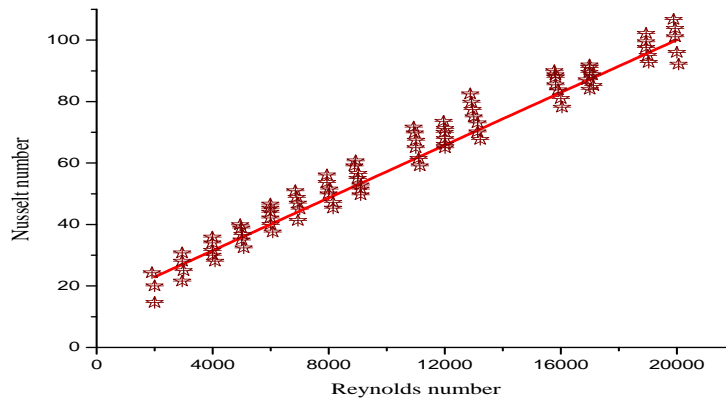


Fig. 16. Variation of Nusselt number with Reynolds number.

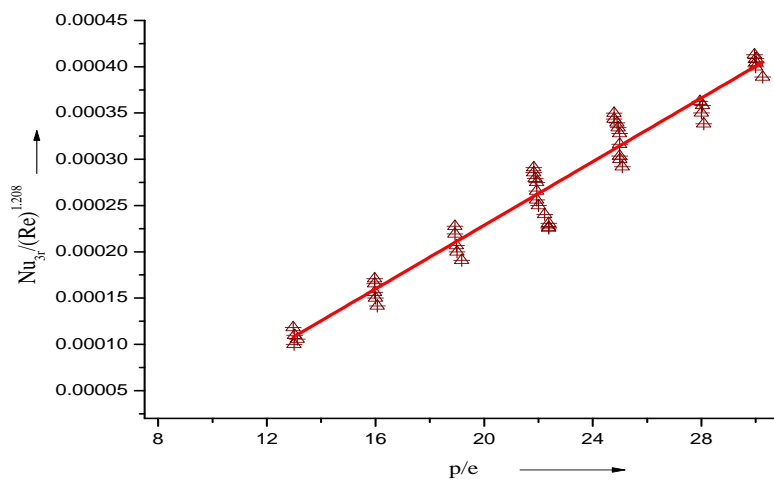


Fig. 17 Plot of $\frac{Nu_{3r}}{(Re)^{1.208}}$ Vs p/e .

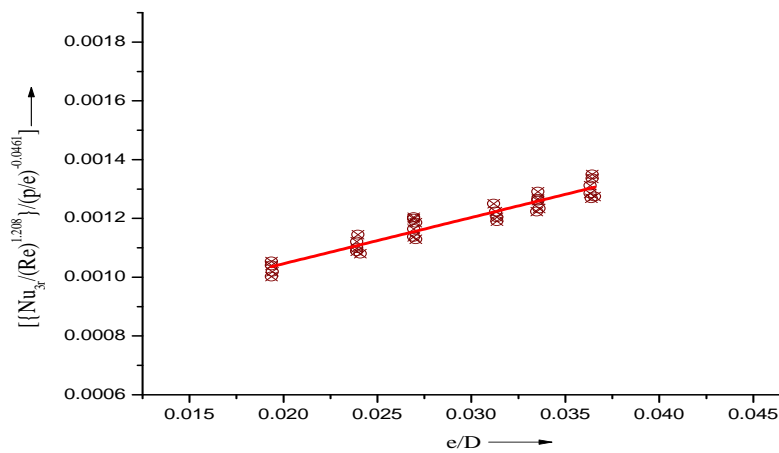


Fig. 18. Plot of $\frac{Nu_{3r}}{(Re)^{1.208}} / (p/e)^{-0.0461}$ Vs e/D .

6.2 Correlation for Nusselt Number of Three Sides Glass Covered Smooth Solar Air Heater

As mentioned earlier in Eq. (9), Nusselt number of smooth solar air heaters is the function of Prndtl number (P_r), Smooth friction factor (f_s) and flow Reynolds number (Re), and hence, to determine the functional relationship between the flow Reynolds number and Nusselt number for smooth duct, all the experimental values of flow Reynolds number were plotted against all the experimental value of Nusselt number, as shown in Fig. 19. The regression analysis method has been utilized to determine the functional equation, written under as:

$$Nu_s = A_1 (Re)^{0.932} \tag{15}$$

Where, A_1 is the function of P_r $\left[A_1 = \frac{Nu_s}{(Re)^{0.932}} \right]$, is plotted against all the experimental values of P_r , as shown in Fig. 20.

The regression analysis to fit a straight line through these points has been given by:

$$\frac{Nu_s}{(Re)^{0.932}} = B_1 (P_r)^{0.5} \tag{16}$$

Where, B_1 is the function of f_s . $\left[B_1 = \frac{\frac{Nu_s}{(Re)^{0.932}}}{(P_r)^{0.5}} \right]$, is

plotted against entire experimental values of f_s , as shown in Fig. 21. The regression analysis to fit a straight line through these points, yield the following correlation for Nusselt number of three sides glass covered smooth solar air heaters :

$$Nu_s = 0.0782 (P_r)^{0.5} (f_s)^{0.7} (Re)^{0.932} \tag{17}$$

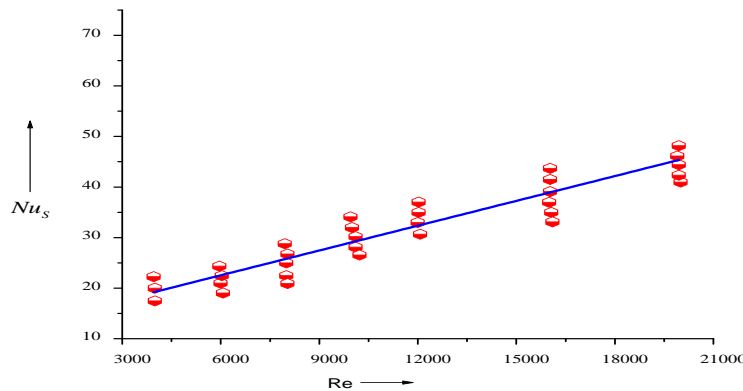


Fig. 19. Nusselt number Vs flow Reynolds number for smooth solar air heater.

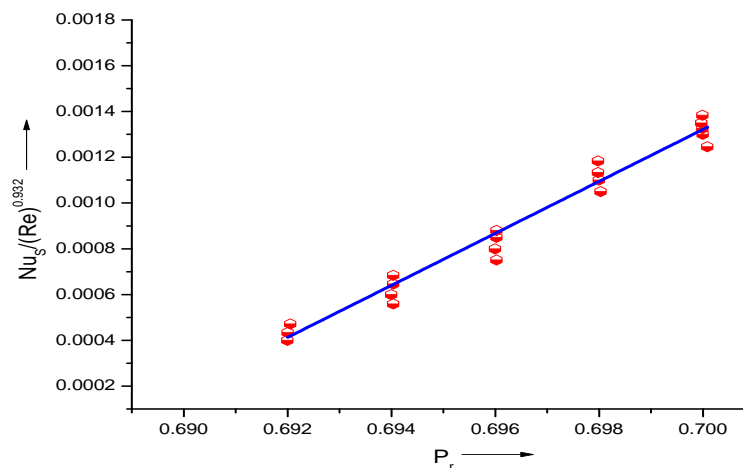


Fig. 20. Plot of $\frac{Nu_s}{(Re)^{0.932}}$ Vs P_r .

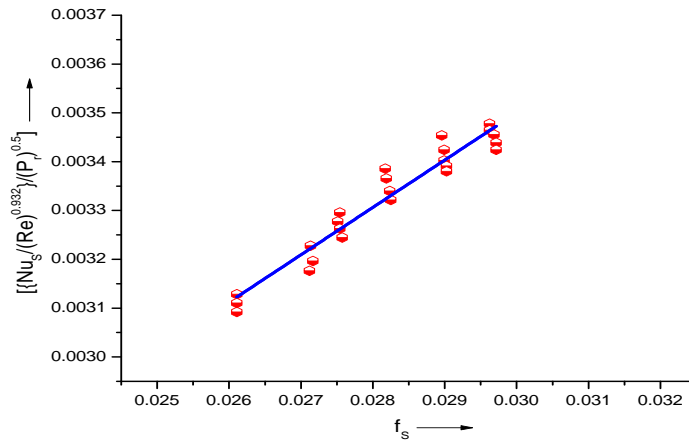


Fig. 21. Plot of $\frac{Nu_s}{(Re)^{0.932}} / (p/e)^{0.5}$ Vs f_s .

6.3 Correlation for Friction Factor of Three Sides Roughened and Glass Covered Solar Air Heater

For the determination of functional relationship between the flow Reynolds number and friction factor, all the experimental values of flow Reynolds number were plotted against all the experimental value of friction factor, as shown in Fig.22. The regression analysis method has been utilized to determine the functional equation, written under as:

$$f_{3r} = A_2 (Re)^{-1.76} \tag{18}$$

Where, A_2 is the function of e/D . $\left[A_2 = \frac{f_{3r}}{(Re)^{-1.76}} \right]$, is plotted against all the experimental values of p/e , as shown in Fig. 23. The regression analysis to fit a straight line through these points has been given by:

$$\frac{f_{3r}}{(Re)^{-1.76}} = B_2 (p/e)^{-0.319} \tag{19}$$

Where, B_2 is the function of e/D .

$$\left[B_2 = \frac{f_{3r}}{(Re)^{-1.76}} / (p/e)^{-0.319} \right], \text{ is plotted against entire}$$

experimental values of e/D , as shown in Fig. 24. The regression analysis to fit a straight line through these points, yield the following correlation for Nusselt number of three sides glass covered smooth solar air heaters :

$$f_{3r} = 0.372 (p/e)^{-0.319} (e/D)^{0.354} (Re)^{-1.76} \tag{20}$$

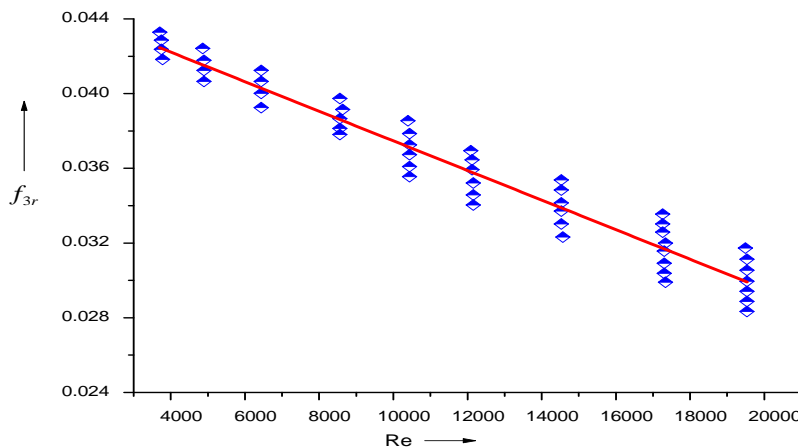


Fig. 22. Variation of friction factor with Reynolds number.

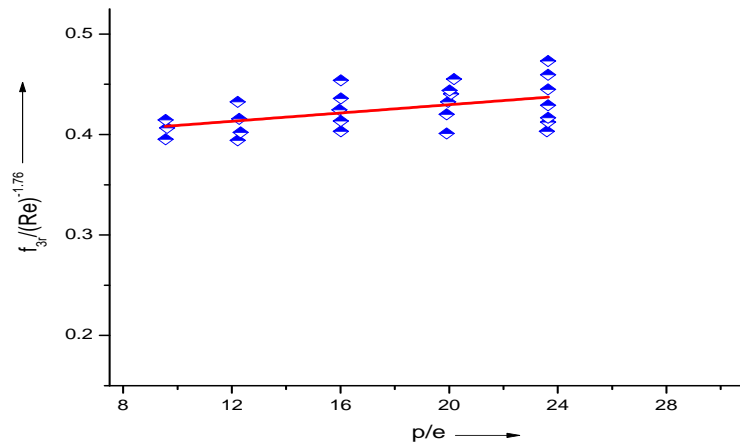


Fig. 23. Plot of $\frac{f_{3r}}{(Re)^{1.76}}$ Vs p/e .

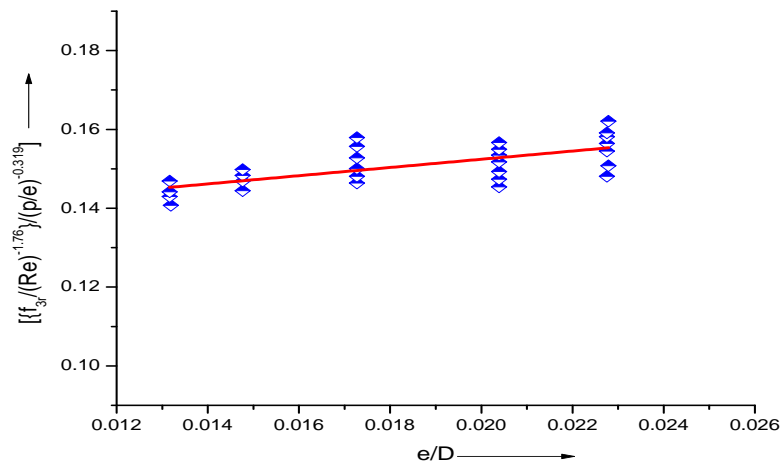


Fig. 24. Plot of $\frac{f_{3r}}{(Re)^{1.76}} / (p/e)^{0.319}$ Vs e/D .

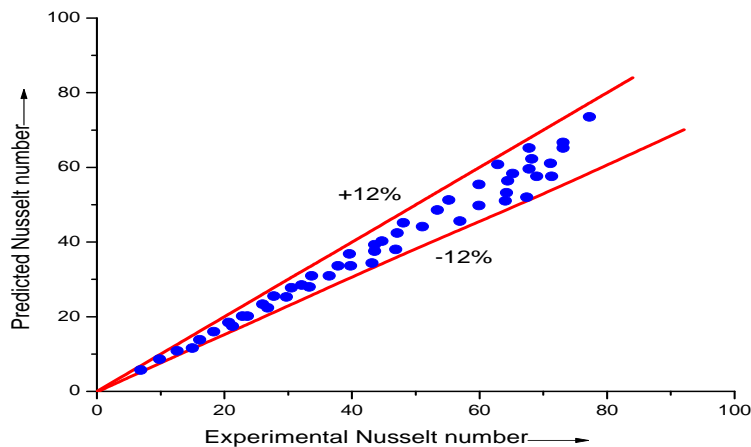


Fig. 25. Comparison of experimental Nusselt number values to the Predicted ones.

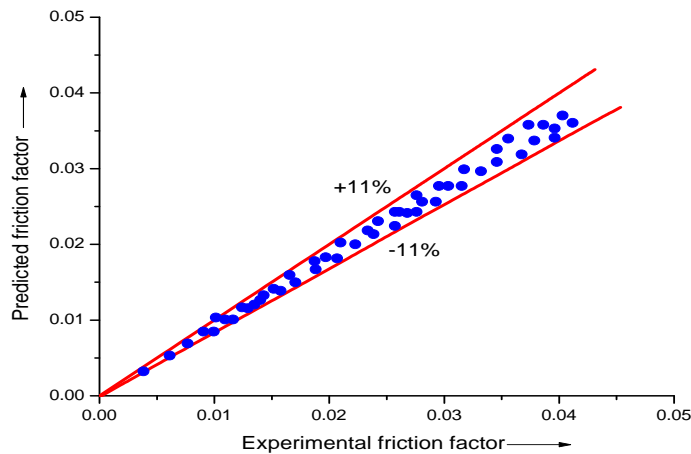


Fig. 26. Comparison of experimental friction factor values to the Predicted ones.

It can be seen from Figs. 25 and 26, that the experimental values of the Nusselt number and friction factor compare well with that of the predicted ones with the average deviations of $\pm 12\%$ and $\pm 11\%$, respectively, which are within the acceptable limit.

Hence, the correlations developed are reasonably satisfactory for the prediction of Nusselt number and friction factor values in three sides artificially roughened and glass covered solar air heaters.

VII. CONCLUSIONS

On the basis of an extensive experimental results for three sides roughened and glass covered solar air heater, the following major conclusions have been observed:-

1. The maximum enhancement achieved in the values of Nusselt number and friction factor were found at relative roughness height (e/D) equal to 0.025 and relative roughness pitch (p/e) equal to 10.
2. The values of Nusselt number in three sides roughened and glass covered solar air heater enhanced by 60%-114% as that of three sides glass covered smooth solar air heater.
3. The values of friction factor in three sides roughened and glass covered solar air heater enhanced by 28%-38% as that of three sides glass covered smooth solar air heater.
4. Correlations of Nusselt number and friction factor for three sides roughened and glass covered solar air heater have been developed. The average deviations between the experimental values and the predicted ones were found to be $\pm 12\%$ and $\pm 11\%$, respectively, which are within the acceptable limit.

REFERENCES

[1] A. K. Behura, B. N. Prasad, L. Prasad, "Heat transfer, friction factor and thermal performance of three sides artificially roughened solar air heaters," *Solar Energy*, vol. 130, pp. 46-59, 2016.
 [2] A. K. Behura, S. K. Rout, H. Pandya, and A. Kumar, "Thermal analysis of three sides artificially roughened solar air heaters," *Energy Procedia*, vol. 109, pp. 279-285, 2017.

[3] B. Bhushan and R. Singh, "Thermal and thermo hydraulic performance of roughened solar air heater having protrude absorber plate," *Solar Energy*, vol. 86, pp. 3388-3396, 2012.
 [4] F. Chabane, N. Moummi, and S. Benramache, "Experimental study of heat transfer and thermal performance with longitudinal fins of solar air heater," *Journal of Advanced Research*, vol. 5, pp. 183-192, 2014.
 [5] S. Chamoli, N. S. Thakur, and J. S. Saini, "A review of turbulence promoters used in solar thermal system," *Renewable and Sustainable Energy Reviews*, vol. 16, pp. 3154-3175, 2012.
 [6] V. B. Gawande, A. S. Dhoble, and D. B. Zodpe, "Effect of roughness geometries on heat transfer enhancement in solar thermal systems- a review," *Renewable and Sustainable Energy Reviews*, vol. 32, pp. 347-378, 2014.
 [7] V. S. Hans, R. P. Saini, and J. S. Saini, "Heat transfer and friction factor correlations for a solar air heater duct roughened artificially with multiple V-ribs," *Solar Energy*, vol. 84, pp. 898-911, 2010.
 [8] J. P. Holman, *Experimental Methods for Engineers*, McGraw Hill Book Company, New York, 2007.
 [9] A. M. Lanjewar, J. L. Bhagoria, and R. M. Sarviya, "Experimental study of augmented heat transfer and friction factor in solar air heater with different orientation of W-Rib roughness," *Experimental Thermal and Fluid Science*, vol. 35, pp. 986-995, 2011.
 [10] A. Kumar, B. N. Prasad, and K. D. P. Singh, "Thermal and thermo hydraulic performance of three sides artificially roughened solar air heaters," *International Research Journal of Advanced Engineering and Science*, vol. 2, issue 2, pp. 215-231, 2017.
 [11] A. Kumar, B. N. Prasad, and K. D. P. Singh, "Enhancement of collector performance parameters in three sides artificially roughened solar air heater," OP Jindal University, Conference Proceedings.4-6 March, 2016.
 [12] A. Kumar, B. N. Prasad, and K. D. P. Singh, "Performance characteristics of three sides glass covered smooth solar air heaters," *Transylvanian Review*, vol. 24, issue 11, pp. 3247-3256, 2016.
 [13] M. J. Lewis, "Optimizing the thermo hydraulic performance of rough surfaces," *International Journal of Heat and Mass Transfer*, vol. 18, pp. 1243-1248, 1975.
 [14] B. N. Prasad and J. S. Saini, "Effect of artificial roughness on heat transfer and friction factor in a solar air heater," *Solar Energy*, vol. 41, pp. 555-560, 1988.
 [15] B. N. Prasad, "Thermal performance of artificially roughened solar air heaters," *Solar Energy*, vol. 91, pp. 59-67, 2013.
 [16] B. N. Prasad and J. S. Saini, "Optimal thermo-hydraulic performance of artificially roughened solar air heaters," *Solar Energy*, vol. 47, pp. 91-96, 1991.
 [17] B. N. Prasad, A. K. Behura, and L. Prasad, "Fluid flow and heat transfer analysis for heat transfer enhancement in three sided artificially roughened solar air heater," *Solar Energy*, vol. 105, pp. 27-35, 2014.

- [18] B. N. Prasad, A. Kumar, and K. D. P. Singh, "Optimization of thermo hydraulic performance in three sides artificially roughened solar air heaters," *Solar Energy*, vol. 111, pp. 313-319, 2015.
- [19] A. Priyam and P. Chand, "Thermal and thermo hydraulic performance of wavy finned absorber solar air heater," *Solar Energy*, vol. 130, pp. 250-259, 2016.
- [20] R. P. Saini and J. Verma, "Heat transfer and friction correlations for a duct having dimple shape artificial roughness for solar air heater," *Energy*, vol. 33, pp. 1277-1287, 2008.
- [21] S. K. Saini and R. P. Saini, "Development of correlations for Nusselt number and friction factor for solar air heater with roughened duct having arc-shaped wire as artificial roughness," *Solar Energy*, vol. 82, pp. 1118-1130, 2008.
- [22] S. Saurav and M. M. Sahu, "Heat transfer and thermal efficiency of solar air heater having artificial roughness: A review," *International Journal of Renewable Energy Research*, vol. 3, pp. 498-508, 2013.
- [23] U. Shakya, R. P. Saini, and M. K. Singhal, "A review on artificial roughness geometry for enhancement of heat transfer and friction characteristics on roughened duct of solar air heater," *International Journal of Emerging Technology and Advanced Engineering*, vol. 3, pp. 279-287, 2013.
- [24] N. Sheriff and P. Gumley, "Heat transfer and friction properties of surfaces with discrete roughness," *International Journal of Heat and Mass Transfer*, vol. 9, pp. 1297-1320, 1966.
- [25] Varun, R. P. Saini, and S. K. Singal, "A review on roughness geometry used in solar air heaters," *Solar Energy*, vol. 81, pp. 1340-1350, 2007.
- [26] Varun, R. P. Saini, and S. K. Singal, "Investigation on thermal performance of solar air heaters having roughness element as a combination of inclined and trasverse ribs on the absorber plate," *Renewable Energy*, vol. 33, pp. 1398-1405, 2008.
- [27] R. L. Webb and E. R. G. Eckert, "Application of rough surfaces to heat exchanger design," *International Journal of Heat and Mass Transfer*, vol. 15, pp. 1647-1658, 1977.
- [28] A. S. Yadav and J. L. Bhagoria, "A CFD (computational fluid dynamics) based heat transfer and fluid flow analysis of a solar air heater provided with circular trasverse wire rib roughness on the absorber plate," *Energy*, pp. 1-16, 2013.